

Paper:

Stability Analysis of Slopes with Terraced Topography in Sapa, Northern Vietnam: Semi-Infinite Slope Assumption with Specific Lengths for Slope Failure

Akihiko Wakai^{*1,†}, Akino Watanabe^{*1}, Nguyen Van Thang^{*1}, Takashi Kimura^{*2},
Go Sato^{*3}, Kazunori Hayashi^{*4}, Nanaha Kitamura^{*1}, Takatsugu Ozaki^{*1},
Hoang Viet Hung^{*5}, Nguyen Duc Manh^{*6}, and Tran The Viet^{*5}

^{*1}Gunma University

1-5-1 Tenjincho, Kiryu, Gunma 376-8515, Japan

[†]Corresponding author, E-mail: wakai@gunma-u.ac.jp

^{*2}Ehime University, Ehime, Japan

^{*3}Teikyo Heisei University, Tokyo, Japan

^{*4}Okuyama Boring Co., Ltd., Miyagi, Japan

^{*5}Thuyloi University, Hanoi, Vietnam

^{*6}University of Transport and Communications, Hanoi, Vietnam

[Received December 1, 2020; accepted January 28, 2021]

Numerous annual slope failures are induced by heavy rainfall during the monsoons, especially in developing countries in Asia. The authors have developed a simple method to predict rising groundwater levels in natural slopes at a relatively shallow depth based on parametric studies conducted using the finite element method. An assumption of a semi-infinite homogeneous slope was adopted in the analysis. Additionally, the authors numerically modelled the vertical infiltration and the lateral seepage flow. Using this method implies that the finite element analysis is not mandatory in the evaluations of practical slopes. Such a simplified approach helps avoid time-consuming tasks in rigorous computations. However, a semi-infinite assumption used in the developed method may provide us with unsuitable solutions, particularly in cases where the slopes include heavily terraced topography with local small cliffs, because theoretically, the first slope failure tends to occur in steep slopes, like the edge of a rice terrace, even though they are very small cliffs. Nevertheless, these local solutions do not affect the conclusions for disaster risk reduction. Moreover, such unsuitable alternatives must be eliminated during analysis. To address this matter, the current study proposes a novel concept of specific lengths. This procedure provides a representative length within the specified length range. The averaged slope gradient is defined by focusing on the secant lines between each topographical grid, while those defined outside the specified range – for example, local cliff angles – are ignored in the slope stability calculation. Consequently, the proposed concept was confirmed to be efficient and can be applied to evaluate the terraced rice fields in Sapa, northern Vietnam. In the past, this area had experienced rainfall-induced slope failures; hence, the

proposed method may be able to simulate these occurrences. The proposed concept's effectiveness when applied to terraced fields should continue to be verified through case studies conducted in areas with extensive small terraced topography.

Keywords: slope failure, heavy rainfall, stability analysis, terraced topography, specific lengths concept

1. Introduction

The mitigation of rainfall-induced slope disasters is a critical issue in Asian countries. Usually, analyzing hydrologic characteristics and slope stability for the risk assessment of slope failure requires accurate rainfall data. In Japan, a nationwide high-density network of high-performance X-band polarimetric radar stations with high resolution and quasi real-time observation capabilities is used to measure rainfall. Recently, approaches for the risk assessment of landslides using weather radar data have been proposed, particularly those providing quick results [1, 2]. Such near-real-time risk assessment has become a global trend [3].

Thus far, the authors have developed a simple method for predicting groundwater rise in natural slopes at a relatively shallow depth. This method is based on parametric studies conducted using the finite element method, assuming a semi-infinite homogeneous slope [4]. This paper elaborates a few technical issues in applying the developed method to a landslide case observed in rice terraces in Vietnam.



2. Simple Evaluation Method for Slope Failure Due to Heavy Rainfall

2.1. Seepage Flow Analysis

The most influential factor on the slope stability is the groundwater level in the slope. The prediction of increasing pore water pressure caused by the rainfall infiltration is required to evaluate slope stability. In our previous works, we assumed that the groundwater flow can be separated into two components: the vertical infiltration and the lateral seepage flow in the slope. To conduct the numerical calculations of across a vast area, a simple calculation model is required to replace the rigorous finite element analysis requiring a high-performance computing environment. Thus, in our previous studies, a novel simplified method was built [4]. The proposed method is based on a simple difference calculation and does not use any nonlinear iterative algorithms required in the finite element method. Such a light calculation load can be advantageous for applications in developing countries. Using the proposed method, real-time slope stability evaluation can be realized employing a large amount of observed rainfall distribution data without high-performance computers. In the future, research based on this perspective needs to be developed, but since this study does not contain observation of rainfall, these details will not be addressed. In this paper, an idea will be proposed for sophisticated slope stability analysis to be performed post-seepage flow analysis.

2.2. Slope Stability Analysis

Once the groundwater level is obtained, the stability of the slope is evaluated by the total factor of safety F_s , implying instability when it is lower than 1.0. By using this index and based on the result of the seepage analysis, the slope stability evaluation can be achieved. As shown in **Fig. 1**, F_s for shallow slope failures assuming a semi-infinite homogeneous slope is defined as

$$F_s = \frac{\tau_f}{\tau} = \frac{c' + \{\gamma \cdot h_1 + (\gamma_{sat} - \gamma_w) \cdot h_2\} \cdot \cos^2 \theta \cdot \tan \phi'}{(\gamma \cdot h_1 + \gamma_{sat} \cdot h_2) \cdot \sin \theta \cdot \cos \theta}, \quad (1)$$

where τ is the shear stress due to the sliding direction component of the gravity of soil, and τ_f is the shear strength of soil, that is, the maximum shear resistance. γ is the wet unit weight of soil, γ_{sat} is the saturated unit weight of soil, γ_w is the unit weight of water, h_1 is the depth from the ground surface to the groundwater level, h_2 is the depth from the groundwater level to the slip surface corresponding to the surface of the base layer, θ is the slope inclination angle, c' is the cohesion of soil, and ϕ' is the angle of shear resistance of soil.

Here, a viable option is performing the slope stability analysis without the previously mentioned seepage flow analysis. To overcome the lack of observed rainfall data at this time, it may be possible to adopt the simple assumption that the groundwater level reaches the ground surface

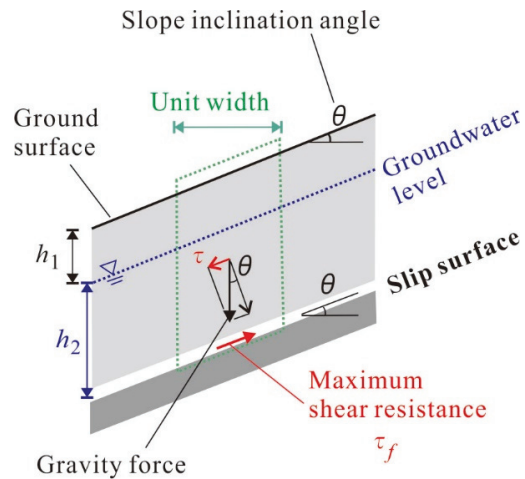


Fig. 1. Slope stability analysis for shallow failures assuming a semi-infinite homogeneous slope.

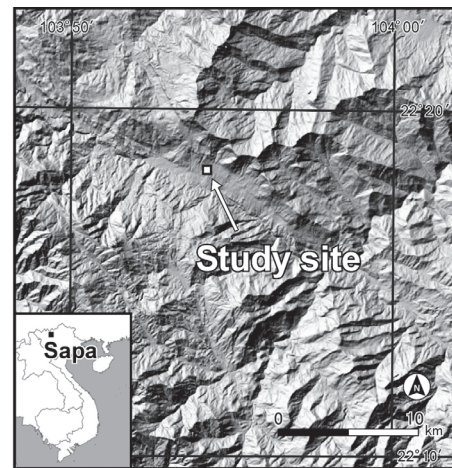


Fig. 2. Location of study area: Sapa Town, Lao Cai Province, Vietnam.

during slope failure. This assumption will be adopted in the case studies presented in the next section.

3. A Case Study in Terraced Rice Fields Slope in Sapa, Vietnam

Every year in the rainy season, landslides frequently occur in Vietnam, particularly in the northern mountainous regions [5–8]. In 2019, some landslides occurred near the Sapa Ancient Rock Field in Hau Thao commune, Sapa Town, Lao Cai Province (**Fig. 2**). As shown in **Fig. 3(a)**, the mountain surface is primarily terraced rice fields belonging to the local Hmong people. The entire slope is a stepped terrain separated by individual rice terraces. **Fig. 3(b)** shows a typical shallow failure case observed in this area, where the length and the width of the sliding block in a plan view was about 30 m and 15 m, respectively. Clearly observable in the slope is a collapsed portion across a few rice terraces. Giao and Hanh [8] noted



(a) Typical terraced rice field



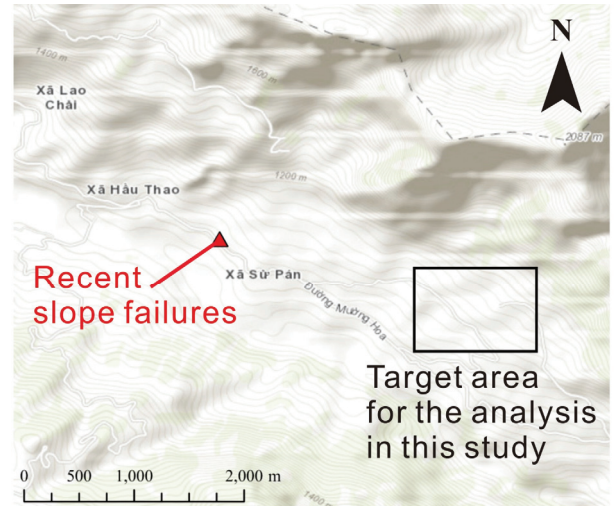
(b) A recent shallow slope failure across a few terraces

Fig. 3. Rice terraces in study area in Sapa Town, Lao Cai Province, Vietnam.

the geology of a landslide, approximately 400 m northwest of the landslide depicted in **Fig. 3(b)**. It consists of a 0.5–0.7 m thick organic top-soil layer, a residual soil layer of 1.4–21.13 m in thickness, and layers of weathered rock underneath. This study also indicated that the geology in the area has a soft soil layer located at a depth of 5 to 7 m, along which a transitional landslide may occur.

3.1. Target Area

Figure 4 shows the target area of the slope stability analysis, which is a rectangular area of around 1,200 m × 800 m, approximately 2 km east of the location of the slope failure, as shown in **Fig. 3(b)**, where the typical topography of terraced rice field is distributed. Although the slope failure should be included in the target area, to obtain the digital elevation model, the authors were forced to change the original target area. In the analysis demonstrated in the following sections, the satellite image AW3D will be used to create the digital elevation model with 1-m resolution. However, the acquired satellite data remains unclear due to the influence of clouds in the area, including the slope failure of **Fig. 3(b)**. However, sufficient data has been obtained in other areas. Inevitably, the adjacent area was selected as the target excluding the slope failures. The collapsed slope is not included in the analysis, but the purpose of our study will be achieved because a district includes a group of slopes with almost the same conditions.



Sources: Esri, HERE, Garmin, Intermap, increment P Corp., GEBCO, USGS, FAO, NPS, NRCAN, GeoBase, IGN, Kadaster NL, Ordnance Survey, Esri Japan, METI, Esri China (Hong Kong), (c) OpenStreetMap contributors, and the GIS User Community

Fig. 4. Positional relationship between the analysis target area and recent slope failures shown in **Fig. 3(b)**.

3.2. Specific Lengths Concept

The semi-infinite assumption used in the developed method may provide us with unsuitable solutions in cases where the slopes consist of a vast terraced topography with local small cliffs, similar to this area. Based on the slope stability theory for shallow failures as shown in **Fig. 1**, the first slope failure tends to occur at a steep part similar to the edge of a rice terrace, even though the cliffs are small. Such unsuitable alternatives must be eliminated. To this end, a new concept is introduced.

Here, the specific lengths concept is proposed to address the problem that theoretically, the edge-like steep part of each rice terrace will always cause the first slope failure. **Fig. 5** is a schematic diagram of the proposed specific lengths concept, elucidating the representative length given within the specific lengths range. The averaged slope gradient is defined by focusing on the secant lines between each topographical grid. The averaged slope gradients defined outside the specific lengths range, for example, local cliff angles, are ignored in the slope stability calculation. As described in **Fig. 1**, the value of the slope inclination θ used for the slope stability analysis can be given as the maximum value of the averaged slope gradients within the specific lengths range. **Fig. 6** is a plan view to show the proposed specific lengths range concept. The central intersection point indicates the position where the representative gradient value is defined. The topographical information of the slope is generally organized as grid data defined in latitude and longitude. The specific lengths are expressed as the diameter of the specific circles in the plan view, providing us the range of possible averaged slope gradients of the representative gradient.

The proposed concept defines not only the lower limit of micro-topography – similar to the resolution of the topography data – but also the upper limit of the calculated length of landslides. As seen in the above points, the pro-

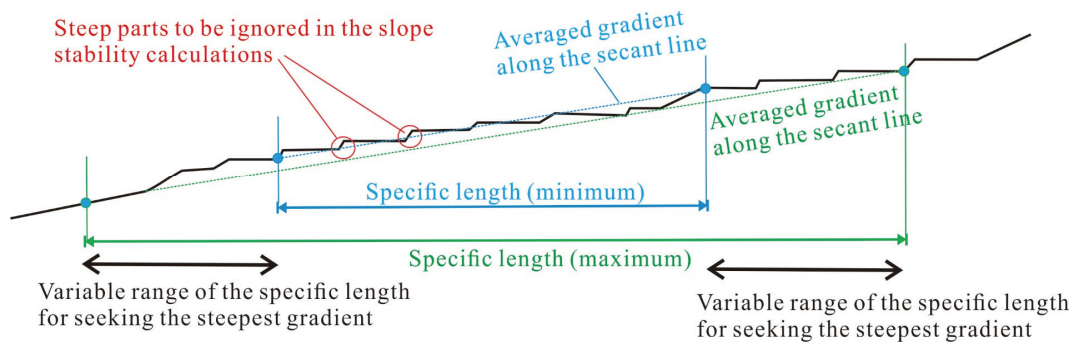


Fig. 5. A schematic diagram of the proposed concept to give a representative length within the specified length range.

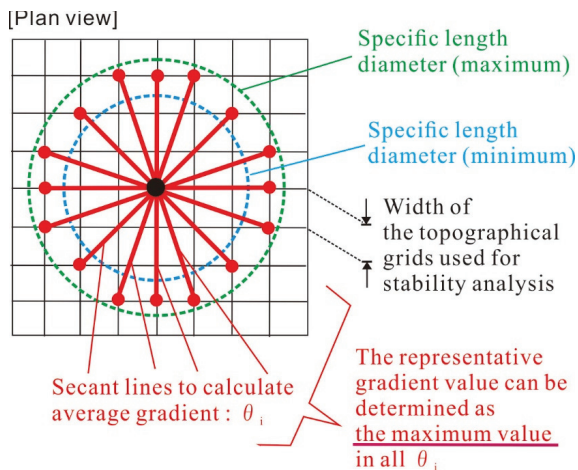


Fig. 6. Plan view of the proposed specific length concept to define the representative gradient used for the stability analysis.

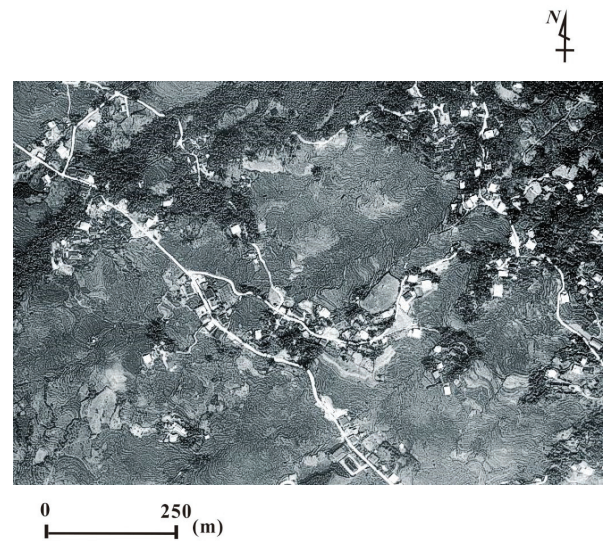


Fig. 7. Aerial photo of the target area of the analysis.

posed concept can be different from simply coarsening the resolution of the digital elevation model. The new concept proposed in this study is thus significant.

3.3. Topographic Analysis

The aerial photo of the target area is shown in **Fig. 7**. The finer folds in the image may correspond to the terraced terrain. **Fig. 8** shows the steepest downward slope at each point, which can be defined as the maximum ground inclination from each pixel to one of its eight neighboring slopes, either adjacent or diagonal. The digital elevation model was provided by the AW3D, a global digital 3D map with 1-m resolution. A pixel here is defined as a point in the grid corresponding to the resolution of the topography. The elevation value of the ground surface at each pixel has been estimated from the satellite data.

In the figure, the darker the color, the greater the angle. If such a simple method is adopted, extremely large angles would be obtained at the edges of individual rice terraces, with the angle inside the rice terraces estimated as approximately zero. Apart from such a simple definition, other methods for defining the slope angle have been comprehensively described in [9]. Examples of detailed

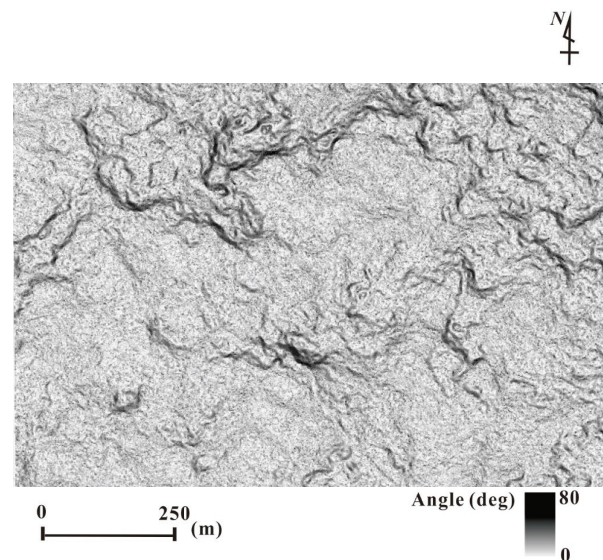


Fig. 8. Distribution of the steepest downward slope angle at each point in the target area based on AW3D.

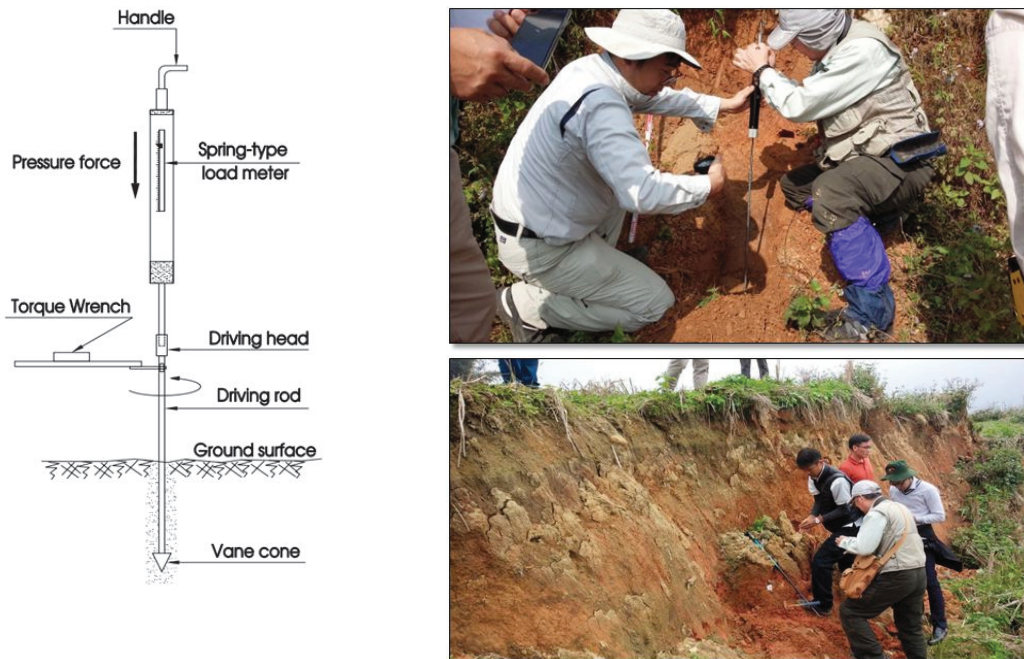


Fig. 9. Vane cone shear test device, named “Dokenbou,” and its operation in the field investigation.

discussions of the definition of micro-topography can be found in the literature, even though they propose an algorithm to calculate the direction of surface water flow different from the central discussion of our study. Further consideration is needed on this point.

3.4. Field Investigation

To understand the nature of typical shallow failures in this area, a simple field investigation at a slope failure was performed in December 2019, as shown in Fig. 3(b). The shear strength parameters of the topsoil were estimated by a convenient and simple device (Fig. 9): the soil-layer-strength measuring instrument (in Japanese, Dokenbou). This device was developed by the Public Works Research Institute of Japan. This instrument has a soil inspection rod, wherein a vane cone is attached to the tip of the rod. The vane cone shear test is conducted by pushing the penetration vane cone to a target depth, with pressure force at a constant value, and shearing the soil by rotating it with a torque wrench. Next, press force and rotation torque values are checked. During each trial, the pressure force was kept constant in a certain level of load. From the measured values, the soil cohesion c' and soil friction angle ϕ' can be easily estimated from the relationship between shear strength and normal stress of soil.

The estimated values are depicted in Table 1. The residual shape of the collapsed slope surface in the longitudinal section is shown in Fig. 10. The depth from the original ground surface to the exposed slip surface H was estimated to be about 5 m. Further studies are required on the effectiveness of such a field investigation.

Table 1. Estimated shear strength parameters of the soil in the topsoil layer based on the results of “Dokenbou.”

c' [kN/m ²]	17.6
ϕ' [°]	35.7

3.5. Analytical Results – Distribution of Calculated Total Factor of Safety

In this study, to assess the potential risk of slope failure in the given area, the total factor of safety F_s for shallow slope failures is used assuming a semi-infinite homogeneous slope, defined as Eq. (1).

Widely known in Japan as empirical knowledge of engineers, the soil cohesion c' and the thickness of the landslide block H have the following approximate relationship [10], except when the thickness of the landslide block is extremely deep (generally more than about 25 m).

$$c' \text{ [kN/m}^2\text{]} = H \text{ [m]}. \quad \dots \dots \dots (2)$$

This equation does not have a theoretical background. Rather, it was developed based on statistical studies of landslide cases for the backward estimation of the value of c' .

Here, as shown in Fig. 3(b), the depth H of the slip surface of the actual slope failure case was observed to be around 5 m. If Eq. (2) is directly adopted in the analysis, c' can be estimated as 5 kN/m², which is smaller than the observed value based on the field shear test with Dokenbou. This field shear test was performed in fine and dry weather. The observed soil cohesion has possibly increased because of the suction exerted in the topsoil layer. Accordingly, this adjustment can be regarded as ra-

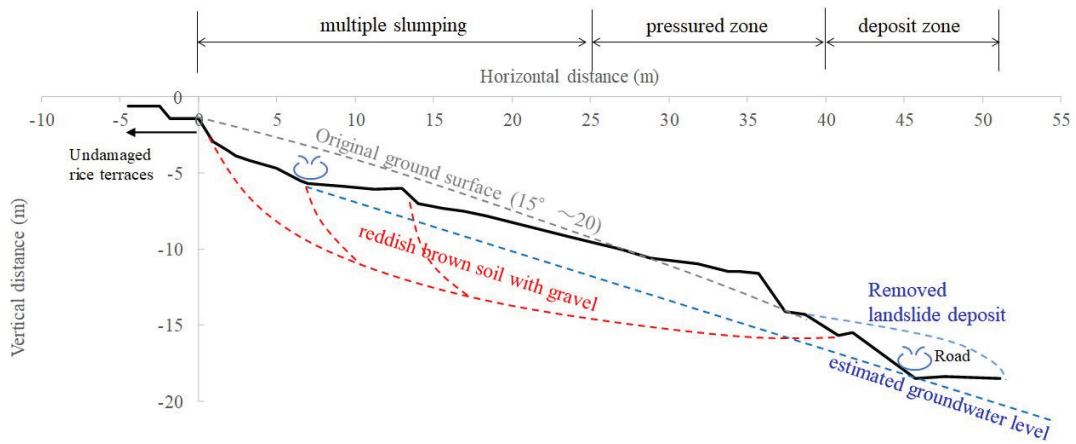


Fig. 10. Residual shape of the collapsed slope surface in the longitudinal section.

Table 2. Analytical parameters used in the slope stability analysis based on the total factor of safety for shallow failures.

γ [kN/m ³]	18.0
γ_{sat} [kN/m ³]	20.0
γ_w [kN/m ³]	9.81
c' [kN/m ²]	5.00
ϕ' [°]	35.7
h_1 [m]	0.00
h_2 [m]	5.00

tional from a mechanical perspective. Therefore, in the analysis, the mobilized c' at the time of slope failure was assumed to be 5 kN/m², based on Eq. (2). Contrariwise, the value of the internal friction angle ϕ' estimated by the Dokenbou may be reliable; thus, in the analysis, it was used in its current condition. As for the unit weights of soil, γ and γ_{sat} , commonly used values were adopted.

In this analysis, the slope inclination angle θ , previously shown in Fig. 8, was used to calculate the total factor of safety at each point. This is the maximum ground inclination from each pixel to one of its eight neighboring grids with 1-m resolutions, either adjacent or diagonal. This is regarded as a conventional method for defining the slope inclination angle. All analytical parameters used in the slope stability analysis are summarized in Table 2.

Figure 11 shows the distribution of calculated total factor of safety at each point. In the figure, the darker the color, the smaller the factor of safety, implying instability. Similar to the tendency in Fig. 8, the dark-colored portions are distributed in a shape like fine folds corresponding to the edges of individual rice terraces. Such a detailed information distribution may not be useful for disaster prevention purposes because collapses of the edges of terraced rice fields do not attract much attention. As demonstrated in Fig. 10, the size of the phenomenon recognized as a slope failure would be more than 10 m at least.

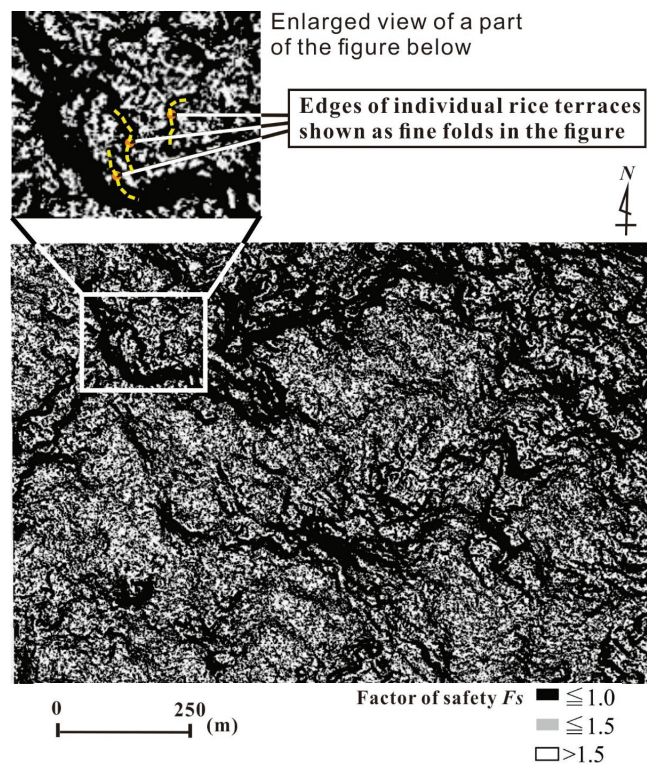


Fig. 11. Distribution of the calculated total factor of safety F_s based on the slope angle θ estimated from the conventional definition as the maximum ground inclination from its eight neighboring grids in 1-m resolution.

3.6. Parametric Study of the Assumed Values of Specific Lengths of Slope Failure

Developing the above result, in this section, the modified results will be demonstrated with the parametric studies by varying the assumed values of the specific lengths of slope failure. The analytical cases are summarized in Table 3. The assumption in Case A would be able to consider extremely local topographical changes – unrealistic from the engineering perspective – while that in Case B

Table 3. Analytical cases for the parametric studies by varying the assumed values of the specific lengths of slope failure.

Case	Specific lengths [m]	
	Minimum	Maximum
A	0	2
B	10	40
C	40	100

is almost consistent with the observed size of an actual slope failure shown in **Fig. 10**. Contrariwise, in **Case C**, the large values of the specific lengths are adopted to capture larger size failures. This assumption may be more suitable for assessing landslides with deeper slip surfaces, for example, 10 m or more.

Figure 12 shows the calculated results in **Case A**. The slope inclination angle was obtained as **Fig. 12(a)**, similar to **Fig. 8**. This is because both assumptions are numerically almost equal. Therefore, **Fig. 12(b)**, obtained based on this inclination angle, tended to be similar to that of **Fig. 11**. As indicated before, under such an assumption, an extremely small total factor of safety was obtained at the edges of individual rice terraces. However, the total factor inside the rice terraces was estimated to be very large. These assumptions may not be desirable.

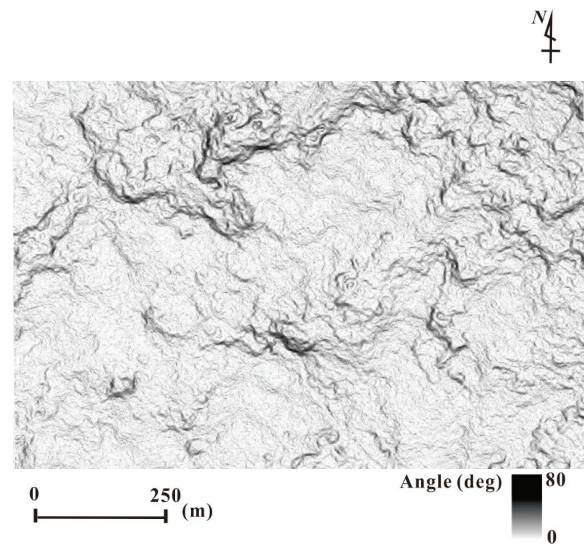
Figure 13 shows the calculated results in **Case B**, where the specific lengths are assumed to be the values consistent with the observed size of an actual slope failure shown in **Fig. 10**. As seen in **Fig. 13(a)**, fine folds with darker color are excluded and only more comprehensive slope shapes are visible. Such modeling seems to be optimal from the engineering point of view, especially when many small-terraced topographies are included in the slope. The calculated result of the total factor of safety shown in **Fig. 13(b)** may also be valid for disaster prevention for shallow slope failures.

However, the danger of large landslides should also be recognized. **Fig. 14** shows the calculated results in **Case C**, where the values of specific lengths may be larger than those in **Case B**. As seen in **Fig. 14(a)**, such a rough pattern characterized with darker colors implies that the target slopes under consideration became larger. **Fig. 14(b)** reminds us which places are more dangerous if a larger landslide occurs. Using these assumptions properly considering the geological structure in the target slope confirmed that by changing the assumed values of the specific lengths of slope failure, various slope objects can be appropriately evaluated.

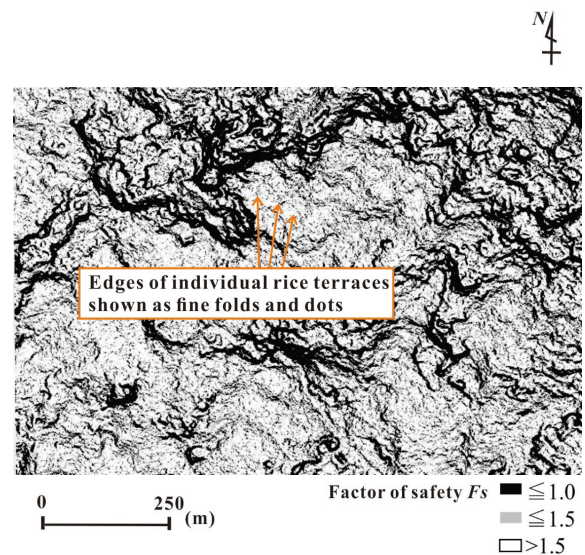
4. Conclusions

The primary results of the present study are as follows:

- (1) Previously, the authors developed a simple method for evaluating the slope stability at a relatively shallow depth. However, it was indicated that such a semi-



(a) Distribution of slope inclination angle



(b) Distribution of total factor of safety

Fig. 12. Calculated results in **Case A** (where the specific lengths range was assumed to be from 0 m to 2 m).

infinite homogeneous slope assumption may provide us with unsuitable solutions in cases where the slopes include highly terraced topography with local small cliffs. This is because theoretically, the first slope failure always occurs at steep slopes like an edge of each rice terrace, even though these are small cliffs. In this study, to address this issue, a new concept of the specific lengths was proposed.

- (2) The proposed specific lengths concept gives a representative length within the specified length range, focusing on the secant lines between each topographical grid. The averaged slope gradients defined outside the specified range are ignored in the slope stability calculation.
- (3) Consequently, it was confirmed that the proposed specific lengths concept is efficient and can be applied

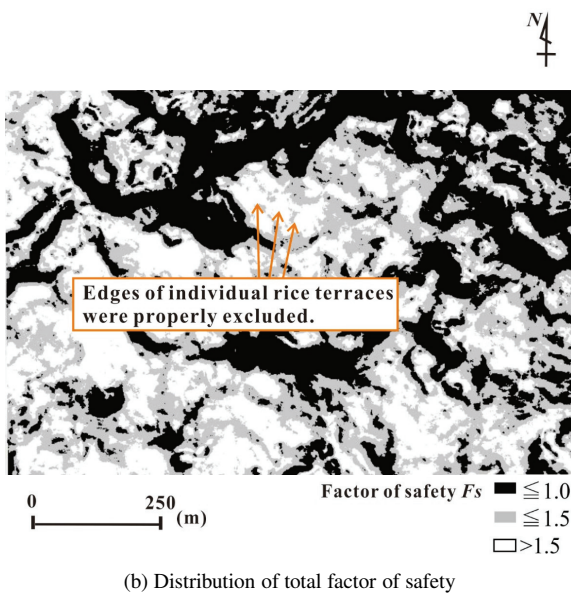
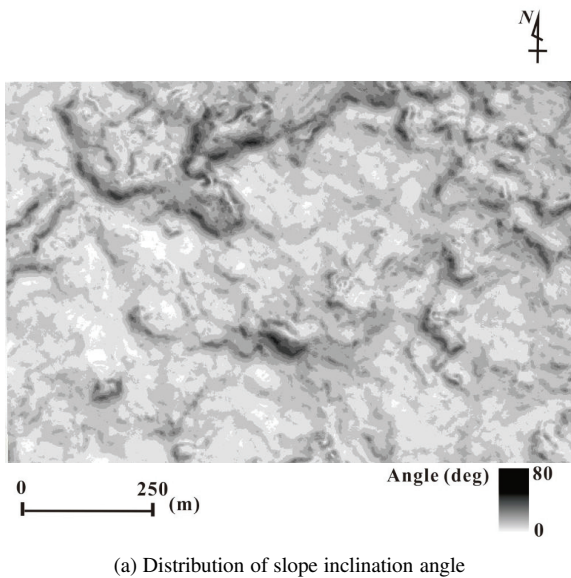


Fig. 13. Calculated results in **Case B** (where the specific lengths range was assumed to be from 10 m to 40 m).

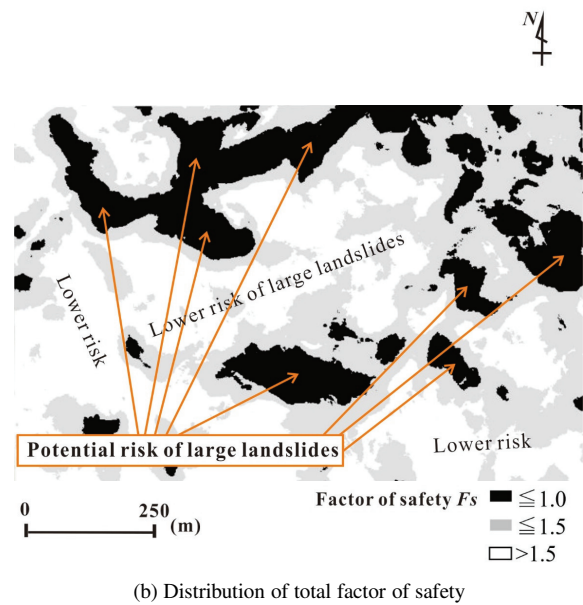
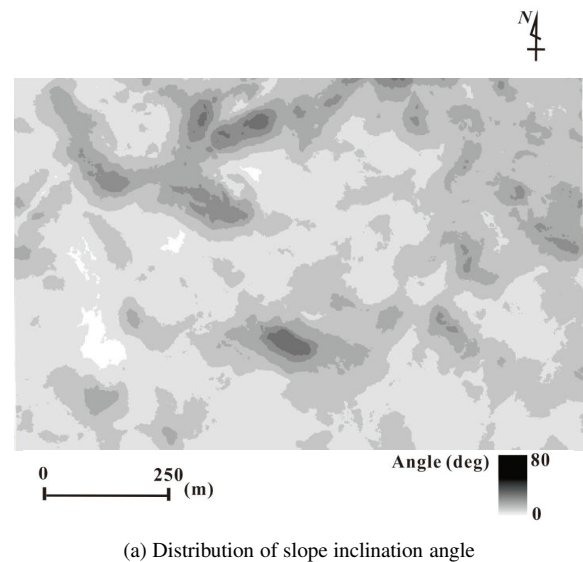


Fig. 14. Calculated results in **Case C** (where the specific lengths range was assumed to be from 40 m to 100 m).

to evaluate the terraced rice fields in Sapa, northern Vietnam.

- (4) To understand the nature of typical shallow failures in this area, a simple field investigation was performed. The shear strength parameters of the soil were estimated by a convenient and simple device called “Dokenbou” in Japanese.
- (5) The effectiveness of the proposed concept for application in terraced fields should continue to be verified through other case studies in different areas with extensive small-terraced topography.
- (6) The proposed concept of specific lengths would be useful for more general slopes including characteristic microtopographies that are relatively unimportant for disaster prevention, similar to the conditions of terraced rice fields studied in this paper.

- (7) In this paper, only simple analytical cases were shown without considering the actual rainfall history. More rigorous stability analysis will be required considering the groundwater level rise based on the actual record of rainfall observed in the target area.

Acknowledgements

This work was supported by JST SICORP, Japan (e-ASIA Joint Research Program) Grant Number JPMJSC18E3, titled as “Establishment of a Landslide Monitoring and Prediction System.” The DEM used in the analysis data is based on AW3D with 1-m accuracy generated from satellite imagery.

References:

- [1] T. Okimura, N. Torii, Y. Osaki, M. Nambu, and K. Haraguchi, "Construction of real-time type hazard system to predict landslides caused by heavy rainfalls," J. of the Japan Society of Erosion Control Engineering, Vol.63, No.6, pp. 4-12, 2011 (in Japanese).
- [2] A. Kinoshita, T. Kanno, A. Okamoto, M. Hitokoto, M. Onodera, M. Sakuraba, and M. Sugiyama, "Construction of real-time hazard map system in Rokko mountain area," J. of the Japan Society of Erosion Control Engineering, Vol.66, No.1, pp. 15-22, 2013 (in Japanese).
- [3] Z. Shi, F. Wei, and V. Chandrasekar, "Radar-based quantitative precipitation estimation for the identification of debris flow occurrence over earthquake-affected regions in Sichuan, China," Natural Hazards and Earth System Sciences, Vol.18, No.3, pp. 765-780, 2018.
- [4] T. Ozaki, A. Watanabe, A. Wakai, and F. Cai, "A simple prediction model for shallow groundwater level rising in natural slopes based on finite element analysis," Proc. of the 4th Int. Conf. on Geotechnics for Sustainable Infrastructure Development, pp. 993-1000, 2019.
- [5] D. Tien Bui, T. A. Tuan, N.-D. Hoang, N. Q. Thanh, D. B. Nguyen, N. Van Liem, and B. Pradhan, "Spatial prediction of rainfall-induced landslides for Lao Cai area (Vietnam) using a hybrid intelligent approach of least squares support vector machines inference model and artificial bee colony optimization," Landslides, Vol.14, No.2, pp. 447-458, 2017.
- [6] T. V. Tran, V. H. Hoang, H. D. Pham, and G. Sato, "Use of Scoops3D and GIS for the Assessment of Slope Stability in Three-Dimensional: A Case Study in Sapa, Vietnam," Proc. of the Int. Conf. on Innovations for Sustainable and Responsible Mining (ISRM 2020), Vol.2, pp. 210-229, 2020.
- [7] D. M. Nguyen and Q. H. Tran, "Features of large-scale landslide at Hau Thao Area, Sa Pa Town, Lao Cai Province," Proc. of the 4th Int. Conf. on Geotechnics for Sustainable Infrastructure Development, pp. 917-922, 2019.
- [8] P. H. Giao and B. X. Hanh, "Analysis of post-landslide electric imaging data at a site in Sapa, Vietnam," Proc. of the EAGE-GSM 2nd Asia Pacific Meeting on Near Surface Geoscience and Engineering, pp. 1-5, 2019.
- [9] D. G. Tarboton, "A new method for the determination of flow directions and upslope areas in grid digital elevation models," Water Resources Research, Vol.33, No.2, pp. 309-319, 1997.
- [10] M. Watari and S. Kobashi, "Prediction and Countermeasures for Landslides and Slope Failures," Sankaido Publishing, pp. 115-116, 1987 (in Japanese).



Name:
Akihiko Wakai

Affiliation:
Professor, Gunma University

Address:
1-5-1 Tenjincho, Kiryu, Gunma 376-8515, Japan

Brief Career:

1997- Research Associate, Gunma University
1998 Visiting Scientist, Tsinghua University
2008 Visiting Scientist, Imperial College London
2011- Professor, Gunma University

Selected Publications:

- "Numerical Modeling of an earthquake-induced landslide considering the strain-softening characteristics at the bedding plane," Soils and Foundations, Vol.50, No.4, pp. 533-545, 2010.
- "Finite element modelling of a creeping landslide induced by snowmelt groundwater," Proc. of the 4th Regional Symp. on Landslide in the Adriatic-Balkan Region, pp. 53-57, 2019.

Academic Societies & Scientific Organizations:

- Japanese Geotechnical Society (JGS)
- Japan Landslide Society (JLS)
- Japan Society of Civil Engineers (JSCE)

Name:

Akino Watanabe

Affiliation:

Graduate Student, Geotechnical Engineering Laboratory, Department of Environmental Engineering Science, Gunma University

Address:

1-5-1 Tenjincho, Kiryu, Gunma 376-8515, Japan

Name:

Nguyen Van Thang

Affiliation:

Ph.D. Student, Geotechnical Engineering Laboratory, Department of Environmental Engineering Science, Gunma University

Address:

1-5-1 Tenjincho, Kiryu, Gunma 376-8515, Japan

Name:

Takashi Kimura

Affiliation:

Assistant Professor, Graduate School of Agriculture, Ehime University

Address:

3-5-7 Tarumi, Matsuyama, Ehime 790-8566, Japan

Name:

Go Sato

Affiliation:

Professor, Graduate School of Environmental Informations, Teikyo Heisei University

Address:

4-21-2 Nakano, Nakano-ku, Tokyo 164-8530, Japan

Name:

Kazunori Hayashi

Affiliation:

Assistant Manager, Okuyama Boring Co., Ltd.

Address:

13-18-306 Futsukamachi, Aoba-ku, Sendai, Miyagi 980-0802, Japan

Name:

Nanaha Kitamura

Affiliation:

Undergraduate Student, Geotechnical Engineering Laboratory, Department of Environmental Engineering Science, Gunma University

Address:

1-5-1 Tenjincho, Kiryu, Gunma 376-8515, Japan

Name:

Takatsugu Ozaki

Affiliation:

Ph.D. Student, Graduate School of Science and Technology, Gunma University

Address:

1-5-1 Tenjincho, Kiryu, Gunma 376-8515, Japan

Name:

Hoang Viet Hung

Affiliation:

Associate Professor of Geotechnical Engineering, Thuyloi University

Address:

175 Tay Son Street, Dong Da District, Hanoi, Vietnam

Name:

Nguyen Duc Manh

Affiliation:

Associate Professor of Geotechnical Engineering, University of Transport and Communications

Address:

No.3 Cau Giay Street, Lang Thuong Ward, Dong Da District, Hanoi, Vietnam

Name:

Tran The Viet

Affiliation:

Department of Civil Engineering, Thuyloi University

Address:

175 Tay Son Street, Dong Da District, Hanoi, Vietnam
